DiffuGesture: Generating Human Gesture From Two-person Dialogue With Diffusion Models

Weiyu Zhao
Harbin Institute of Technology
Weihai, Shandong, China
weiyuzhao66@gmail.com

Liangxiao Hu
Harbin Institute of Technology
Weihai, Shandong, China
lx.hu@hit.edu.cn

Shengping Zhang*
Harbin Institute of Technology
Weihai, Shandong, China
s.zhang@hit.edu.cn

ABSTRACT

This paper describes the DiffuGesture entry to the GENEA Challenge 2023. In this paper, we utilize conditional diffusion models to formulate the gesture generation problem. The DiffuGesture system generates human-like gestures from the two-person dialogue scenario, which are responsive to the interlocutor motions and accompany with the input speech. DiffuGesture system is built upon the recent DiffGesture [39]. Specifically, we introduce a lightweight transformer encoder to fuse the temporal relationships between human gestures and multi-modal conditions. Moreover, we adopt implicit classifier-free guidance to trade off between diversity and gesture quality. According to the collective evaluation released by GENEA Challenge 2023, our system demonstrates strong competitiveness in the appropriateness evaluation.

CCS CONCEPTS

• **Computing methodologies** → **Animation**; *Neural networks.*

KEYWORDS

gesture generation, diffusion models, neural networks

ACM Reference Format:
Weiyu Zhao, Liangxiao Hu, and Shengping Zhang*. 2023. DiffuGesture: Generating Human Gesture From Two-person Dialogue With Diffusion Models . In *Proceedings of Make sure to enter the correct conference title from your rights confirmation emai (ICMI '23,).* ACM, New York, NY, USA, 7 pages. https://doi.org/XXXXXXX.XXXXXXX

1 INTRODUCTION

Human gestures serve as a distinct mode of communication in daily conversations, which assists the speakers in conveying semantic information more effectively and facilitate interpersonal communication. [21, 29]. Therefore, generating realistic co-speech human gestures from conversations plays a crucial role in achieving improved interaction between virtual entities and humans. Our goal is to generate co-speech human gestures from the two-person dialogue. However, generating human gestures with multi-modal data such as audio, text, and conversational cues in two-person dialogue remains a challenging and unresolved problem.

Early research in data-driven co-speech gesture generation approaches often relies on statistical analysis. Levine [16] et al. utilize probabilistic models to establish the relationship between audio and gestures. In recent years, deep learning methods have been increasingly applied in co-speech gesture generation. Kucherenko [12] et al. and Yoon [34] et al. employ the multi-layer perceptron (MLP) and recurrent neural network (RNN) methods to generate deterministic human gestures, respectively. But these approaches do not adequately address the implicit mapping between the data and gestures [13]. To achieve more diverse and personalized gesture movements and improve the mapping between data and gestures, there emerge methods using GAN [3, 25, 30], diffusion models [27, 32, 39] and VQ-VAE [20, 22].

However, these methods mainly focus on single-person co-speech gesture generation. In this paper, we present a novel approach for co-speech human gesture generation in the two-person dialogue scenario.

Specifically, given the behavior of the interlocutor and the audio and textual transcriptions of the main agent, we generate the reaction and co-speech movements of the main agent, respectively. Inspired by [39], we adopt conditional diffusion models for co-speech gesture generation from two-person dialogue. Specifically, we introduce a lightweight transformer encoder to enhance the contextual relevance between human gestures and multi-modal conditions. Finally, we introduce implicit classifier-free guidance to trade off between diversity and gesture quality.

The main contributions of our work are:

- We present an early attempt to utilize conditional diffusion models for co-speech human gesture generation from two-person dialogue, which generates impressive co-speech gesture movements.
- We introduce a lightweight transformer encoder that effectively fuses the temporal relationships between human gestures and multi-modal conditions.

2 RELATED WORK

In this section, we will discuss the previous work in the fields of gesture generation and diffusion model generation.

2.1 Data-driven Gesture Generation

The data-driven approach to gesture generation has found extensive applications across various domains.In recent years, researchers have utilized audio [6, 17, 18, 22], transcribed text [3, 10, 23, 26, 27, 36], and multimodal data [2, 19, 33] to drive gesture generation. The use of audio-driven gesture generation is quite common in various

*Corresponding author.

Permission to make digital or hard copies of all or part of this work for personal or classroom use is granted without fee provided that copies are not made or distributed for profit or commercial advantage and that copies bear this notice and the full citation on the first page. Copyrights for components of this work owned by others than ACM must be honored. Abstracting with credit is permitted. To copy otherwise, or republish, to post on servers or to redistribute to lists, requires prior specific permission and/or a fee. Request permissions from permissions@acm.org.
ICMI '23,, October 9-13, 2023, Paris, France
© 2023 Association for Computing Machinery.
ACM ISBN 978-1-4503-XXXX-X/18/06…$15.00
https://doi.org/XXXXXXX.XXXXXXX

applications. For example, Ginosaret et al. [6] utilize an adversarial discriminator to regress gestures from audio. Qian et al. [22] employ conditional learning to achieve audio-driven gesture generation, alleviating the ambiguity in simultaneous speech and gesture synthesis. Audio2gestures [18] and DanceFormer [17] use a variational autoencoder [11] and Transformer [28], respectively, to generate gestures from audio. Text-driven motion synthesis can be seen as learning a joint embedding of the text feature space and the motion feature space[22]. Text2gestures [3] establishes the connection between text and gesture actions using a transformer. T2M-GPT [36] and MotionGPT[10], built upon generative pre-trained transformer (GPT), treat gesture actions as a language and utilize VQ-VAE to transform text into gesture actions. MDM [27] and MotionClip [26] preprocess transcribed text using CLIP[23] to establish the conversion between action and text embeddings.

Recently, there has been an increasing trend in co-speech gesture generation to use multimodal data, including audio, text, and speaker id. Yoon et al. [33] proposed a model that combines multimodal context and adversarial training to generate gestures that resemble human-like movements and are synchronized with the speech content and rhythm. Rhythmic Gesticulator [2] is the first model to use neural networks to establish the relationship between gestures and audio in terms of rhythm and semantics. HA2G [19] leverages contrastive learning strategies to fully utilize the rich connections between speech audio, text, and human gestures, resulting in the generation of realistic gesture movements. However, none of the aforementioned works considered the influence of other individuals in dyadic conversations on the embodied agents.

2.2 Diffusion Models

Diffusion models are a type of probabilistic generative model based on stochastic processes [8], where initial data points gradually evolve towards the target distribution through a diffusion process at each time step. Dhariwal et al. [5] introduce classifier guidance to improve sample quality and generate higher-quality results. Then, the introduction of the Classifier-Free Guidance [9] eliminates the need for explicit classification models and supports more open-ended and exploratory generation in various tasks. Diffusion models have recently been widely applied in various fields, such as image generation [24], 3D shape generation [31], video generation [7].

More recently, in the context of gesture generation tasks, diffusion generative models [1, 27, 37, 39] have also been employed for co-speech gesture generation. Inspired by the work of DiffGesture [39] in 2D gesture generation, we have developed a framework for generating 3D gesture poses from multimodal data in a two-person dialogue scenario.

3 METHOD

Given the behavior of the interlocutor and the audio and textual transcriptions of the main agent, our goal is to generate the listening reactions and co-speech motions simultaneously. The architecture of our system is depicted in Figure 1(a). We first introduce the problem definition in Section 3.1. Then we present the diffusion process and reverse process for gesture generation in Section 3.1. Finally, we develop a transformer encoder to fuse the temporal relationships between human gestures and multi-modal conditions in Section 3.3.

3.1 Problem Definition

Given the sequences of 3D full-body motions, we represent them as $x = \{p_1, p_2, p_3, ..., p_n\} \in \mathbb{R}^{N\times 3J}$, N represents the sequence length and J denotes the total joint number. The reverse denoising process G of the diffusion model is parameterized by θ to synthesize the main agent skeleton sequence x_m, which is further conditioned on the multi-modal conditions C and the initial poses of the previous M frames x_{pre}. The learning objective can be expressed as $argmin_\theta \left\| x_m - G_\theta(C, x_{pre}) \right\|$.

3.2 Diffusion-based Gesture Generation

Inspired by the previous work [39], we extend this model in the two-person dialogue scenario. Unlike generating 2D skeletal upper-body poses in [39], we synthesize the full-body human gestures and establish the forward and reverse processes for conditional diffusion models.

Diffusion Process. The diffusion process, also known as the forward process, is used to approximate the posterior distribution $q(x_{1:T}|x_0)$. It gradually introduces Gaussian noise into the original distribution based on the variance sequence $\beta_1, ..., \beta_t$, where $\beta_i \in (0, 1)$. The diffusion process is defined as follows:

$$q(x_t^{1:N}|x_{t-1}^{1:N}) = \mathcal{N}(\sqrt{\beta_t}x_{t-1}^{1:N}, (1-\beta_t)I), \tag{1}$$

$$q(x_{1:T}|x_0) = \prod_{t=1}^{T} q(x_t^{1:N}|x_{t-1}^{1:N}), \tag{2}$$

where $x_t^{1:N}$ represents the main agent motion sequence $\{p_m\}_{i=1}^{N}$ at t denoising step. Next, we will slightly abuse the use of letters and use x to represent $x^{1:N}$. By progressively adding noise in this manner to the original gesture motions x_0, it approaches a distribution that closely resembles white noise.

Reverse Process. The reverse process, also known as the generation process, estimates the joint distribution $p_\theta(x_{0:T})$. The reverse process of diffusion models also maintains the form of Gaussian transition. Additionally, following the idea of classifier-free guidance, we train the model in both unconditional and conditional generation settings to generate more realistic and diverse gesture motions. The reverse process is defined as follows:

$$p_\theta(x_{0:T}) = p_\theta(x_T)\prod_{t=1}^{T} p_\theta(x_{t-1}|x_t, C), \tag{3}$$

$$where \quad p_\theta(x_{t-1}|x_t, C) = \mathcal{N}(x_{t-1}; \mu_\theta(x_t, t, C), \sum_\theta(x_t, t)). \tag{4}$$

Equation 4 represents the conditional generation and we set the conditions C as zero (denoted as ϕ) for unconditional generation in the training stage. The corrupted noisy gesture sequence x_t is sampled by $q(x_t|x_0)$.

Traning loss. According to DDPM [8], the previous corrupted gesture sequence x_{t-1} is defined as follows:

$$x_{t-1} = \frac{x_t - \sqrt{1-\bar{\alpha}_t}\hat{\epsilon}}{\sqrt{\bar{\alpha}_t}}, \tag{5}$$

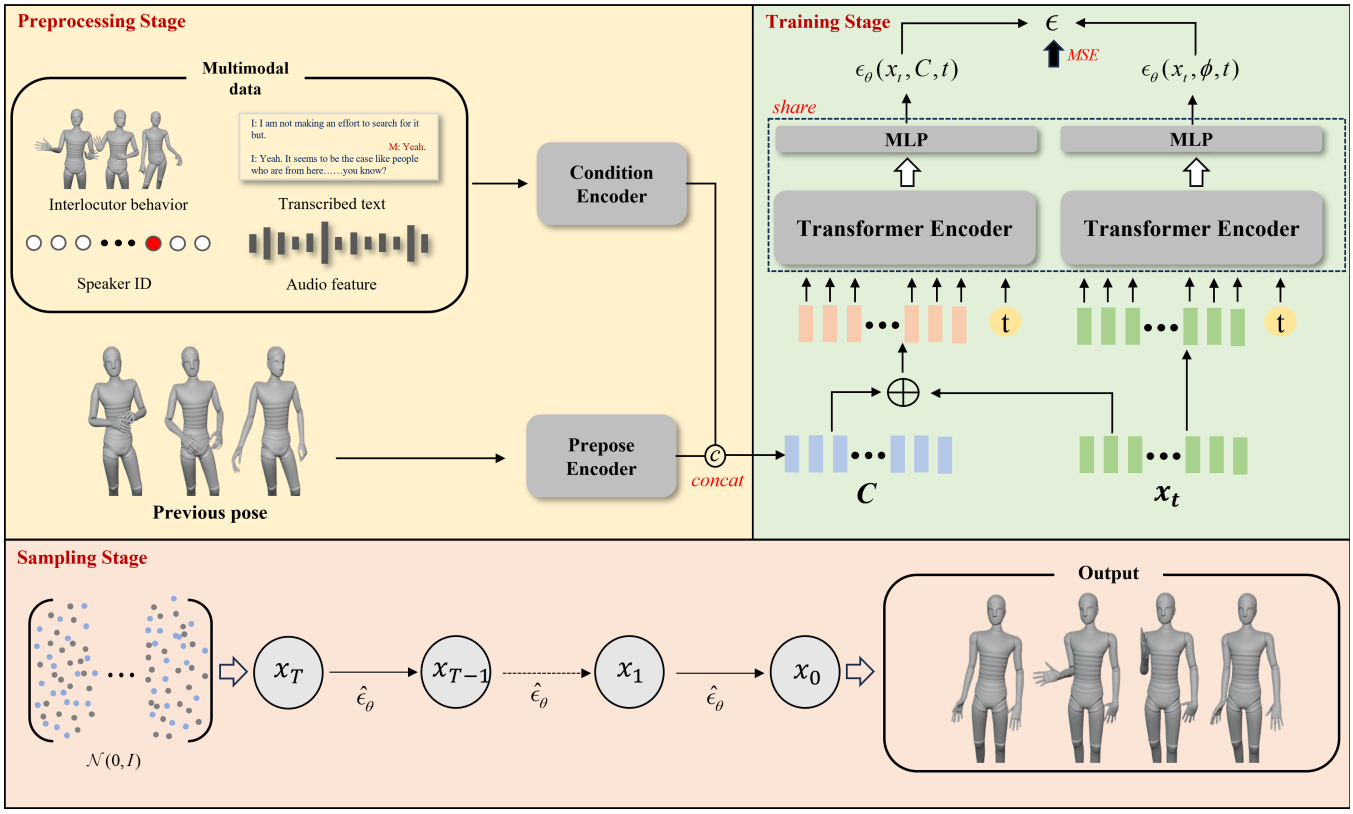

Figure 1: Overview of the Diffu2guesture framwork. In the preprocessing stage (yellow), we develop a condition encoder and a propose encoder to process multi-modal data and previous poses, respectively. Then we concatenate the two outputs together to create condition features C. In the training stage (green), we introduce classifier-free guidance to train the transformer encoder. In the sampling stage (pink), we start with random noise x_T and generate a clean sample x_0 through T denoising steps.

$$where \quad \bar{\alpha}_t = \prod_{i=1}^{t} 1 - \beta_i. \tag{6}$$

So we can denoise the Gaussian noise to the original gesture motion distribution step by step. Then, we use the Mean Squared Error (MSE) loss to compute the loss between the estimated noise and the actual noise at each time step [39]:

$$\mathcal{L}_{simple} = \mathbb{E}_q \left[\left\| \epsilon - \epsilon_\theta(\sqrt{\bar{\alpha}_t} x_0 + \sqrt{1-\bar{\alpha}_t}\epsilon, C, t) \right\|^2 \right]. \tag{7}$$

Where ϵ_θ is the predicted Gaussian noise, and ϵ represents the actual added noise. During the training process, we randomly mask the conditions C for the unconditional setting.

Sampling. Due to the classifier-free guidance, the predicted noise at each step in the sampling stage can be represented as:

$$\hat{\epsilon}_\theta = \epsilon_\theta(x_t, \phi, t) + s \cdot (\epsilon_\theta(x_t, C, t) - \epsilon_\theta(x_t, \phi, t)), \tag{8}$$

where s is the scale parameter to trade off the diversity and quality.

3.3 Cross-Modal Attention Encoding

Generating 3D gesture poses using conditional diffusion models is different from generating images. Both the pose sequence x and the multi-modal conditions C exhibit strong temporal dependencies. Here, we need to establish a module to ensure that our results are time-dependent. Unlike previous work in the GENEA 2022 challenge that utilizes LSTM [4], VQVAE [20], and graph models [38], we employ a lightweight transformer encoder to encode N frames of continuous motions and multi-modal data. We align the noisy gesture sequence x_t and multi-modal conditions C in the time dimension and treat each frame as a separate token. The time step t is treated as a separate token. We then utilize attention mechanisms for encoding.

$$Attention(Q, K, V) = softmax(\frac{QK^T}{\sqrt{d_k}})V. \tag{9}$$

Where Q, K, and V are the query, key, and value matrix from input tokens, in the multi-head attention mechanism.

4 EXPERIMENT

4.1 Data Processing

The only dataset we used is the GENEA Challenge 2023 [14] dataset, which is an extension of Lee et al.'s Talking With Hands [15] dataset. The dataset includes participants consisting of a main agent (tasked with generating motion) and an interlocutor (the other party in the

conversation). The conversation data in the dataset is in dyadic form, providing audio and text transcriptions for both parties, speaker IDs, and motion. In the provided official data, each recorded conversation is duplicated with flipped roles to augment the training data.

We fully leverage the various information available in the dataset, including the audio and transcribed text between the main agent and the interlocutor, as well as the speaker IDs. We follow the same processing approach as the baseline [4] for handling audio, transcriptions, and human body joints. We obtain three audio features at a sampling rate of 44100: mel-spectrograms, MFCCs, and prosodies. The frames generated have a rate of 30 FPS and their length matches the duration of the motion sequence. We encode the text using Fasttext, resulting in word vectors of dimension 300. Additionally, two extra dimensions are used to indicate whether the speaker is silent or laughing. Furthermore, we define the identity information of each speaker using one-hot encoding.

For the processing of motion data, we also select 25 joints, including the root node, which have a significant influence on skeleton motion. These joints are represented in a dimension of 78. To generate high-quality motion sequences, we crop the motion sequence into segments at a rate of 300 frames per second, which serve as inputs to the diffusion process. To ensure continuity between adjacent motion segments, we extract the previous pose at a rate of 50 frames per second as part of the generation condition. After aligning the audio features, encoded text, identity information, and speakers' motion sequence in the temporal dimension, the total dimension of the multimodal conditional data is [300,932]. Similarly, the previous pose is mapped to the corresponding dimension after being processed by the prepose encoder.

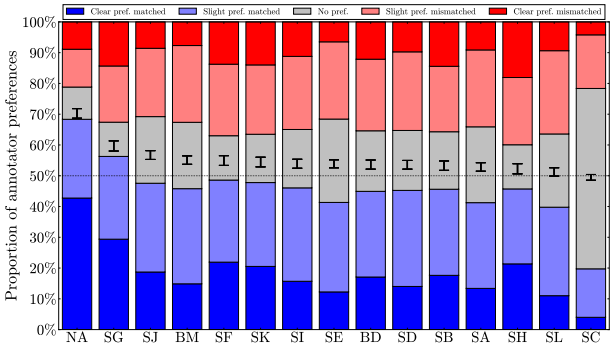

(a) Appropriateness for agent speech

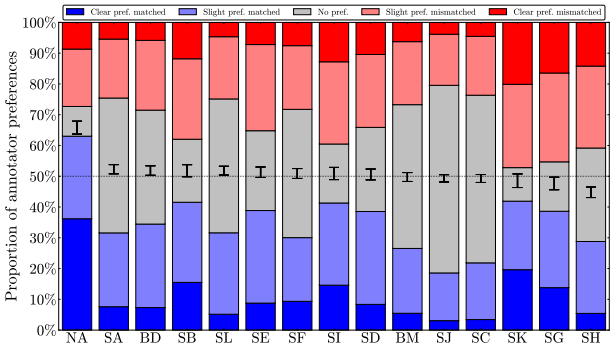

(b) Appropriateness for the interlocutor

Figure 2: The bar plots display response distribution in appropriateness studies. The blue bar represents preferred matched motion responses, and the red bar represents preferred mismatched motion responses. The height of each bar corresponds to the fraction of responses in each category. On top of each bar is also a confidence interval for the mean appropriateness score, scaled to fit the current axes. The dotted black line indicates chance-level performance. Conditions are ordered by mean appropriateness score.

4.2 Evaluation

The evaluation of our approach is conducted through subjective assessment by the organizers of the GENEA Challenge 2023 and other participating teams. The organizers recruit study participants residing in the UK, IE, USA, CAN, AUS, and NZ, who had English as their first language, via crowdsourcing platforms to perform the evaluations. Multiple attention checks are implemented during the experiment to ensure the participants' engagement and attentiveness. The evaluation of this challenge consisted of three aspects: **human-likeness; appropriateness for agent speech; appropriateness for the interlocutor.** The specific results are presented in Table 1 and Table 2. The natural motion is labeled NA. Our method is labeled **SB** in the tables.

Human-likeness. The study participants watch 8 to 10 seconds of video and rate the motion of the virtual character as human-like, independent of the dialogue content and the speaker. DiffuGesture performs poorly on this metric.

Appropriateness for agent speech. This metric evaluates whether the motion of the virtual character is appropriate for the given speech, while controlling for the overall human-likeness of the motion [35]. During the testing process, study participants are presented with a pair of videos, both from the same condition, where one video matches the specific speech and the other is from an unrelated speech. Both videos play the specific speech, and participants are asked to select the video they believe best matches the speech.

Appropriateness for the interlocutor. During the conversation process, both participants in the dialogue influence each other. Therefore, this metric evaluates whether the motion of the virtual character is appropriate for the given interlocutor's behavior (including speech and motion) while controlling for the overall human-likeness of the motion. Study participants are also presented with a pair of videos, where the behavior of the main agent remains fixed, but the behavior of the interlocutor is randomly replaced in one of the videos. Participants are then asked to select the video that best matches the behavior of the interlocutor. DiffuGesture has achieved promising results in this metric.

Table 1: Summary statistics of user-study responses from both appropriateness studies, with confidence intervals for the mean appropriateness score (MAS) at the level $\alpha = 0.05$. "Pref. matched" identifies how often test-takers preferred matched motion in terms of appropriateness after splitting ties. Conditions are ordered by mean appropriateness score.

(a) Appropriateness for agent speech

Condition	MAS	Pref. matched	Raw response count 2	1	0	−1	−2	Sum
NA	0.81±0.06	73.6%	755	452	185	217	157	1766
SG	0.39±0.07	61.8%	531	486	201	330	259	1807
SJ	0.27±0.06	58.4%	338	521	391	401	155	1806
BM	0.20±0.05	56.6%	269	559	390	451	139	1808
SF	0.20±0.06	55.8%	397	483	261	421	249	1811
SK	0.18±0.06	55.6%	370	491	283	406	252	1802
SI	0.16±0.06	55.5%	283	547	342	428	202	1802
SE	0.16±0.05	54.9%	221	525	489	453	117	1805
BD	0.14±0.06	54.8%	310	505	357	422	220	1814
SD	0.14±0.06	55.0%	252	561	350	459	175	1797
SB	0.13±0.06	55.0%	320	508	339	386	262	1815
SA	0.11±0.06	53.6%	238	495	438	444	162	1777
SH	0.09±0.07	52.9%	384	438	258	393	325	1798
SL	0.05±0.05	51.7%	200	522	432	491	170	1815
SC	−0.02±0.04	49.1%	72	284	1057	314	76	1803

(b) Appropriateness for the interlocutor

Condition	MAS	Pref. matched	Raw response count 2	1	0	−1	−2	Sum
NA	0.63±0.08	67.9%	367	272	98	189	88	1014
SA	0.09±0.06	53.5%	77	243	444	194	55	1013
BD	0.07±0.06	53.0%	74	274	374	229	59	1010
SB	0.07±0.08	51.8%	156	262	206	263	119	1006
SL	0.07±0.06	53.4%	52	267	439	204	47	1009
SE	0.05±0.07	51.8%	89	305	263	284	73	1014
SF	0.04±0.06	50.9%	94	208	419	208	76	1005
SI	0.04±0.08	50.9%	147	269	193	269	129	1007
SD	0.02±0.07	52.2%	85	307	278	241	106	1017
BM	−0.01±0.06	49.9%	55	212	470	206	63	1006
SJ	−0.03±0.05	49.1%	31	157	617	168	39	1012
SC	−0.03±0.05	49.1%	34	183	541	190	45	993
SK	−0.06±0.09	47.4%	200	227	111	276	205	1019
SG	−0.09±0.08	46.7%	140	252	163	293	167	1015
SH	−0.21±0.07	44.0%	55	237	308	270	144	1014

Table 2: Summary statistics of user-study ratings from the human-likeness study, with confidence intervals at the level $\alpha = 0.05$. Conditions are ordered by decreasing sample median rating. Our entry is SB.

Condition	Human-likeness Median	Mean
NA	71 ∈ [70, 71]	68.4±1.0
SG	69 ∈ [67, 70]	65.6±1.4
SF	65 ∈ [64, 67]	63.6±1.3
SJ	51 ∈ [50, 53]	51.8±1.3
SL	51 ∈ [50, 51]	50.6±1.3
SE	50 ∈ [49, 51]	50.9±1.3
SH	46 ∈ [44, 49]	45.1±1.5
BD	46 ∈ [43, 47]	45.3±1.4
SD	45 ∈ [43, 47]	44.7±1.3
BM	43 ∈ [42, 45]	42.9±1.3
SI	40 ∈ [39, 43]	41.4±1.4
SK	37 ∈ [35, 40]	40.2±1.5
SA	30 ∈ [29, 31]	32.0±1.3
SB	24 ∈ [23, 27]	27.4±1.3
SC	9 ∈ [9, 9]	11.6±0.9

5 DISCUSSION

We achieve satisfactory results in both the appropriateness for agent speech and appropriateness for the interlocutor metrics, as shown in Table 1. Our scores for these two metrics were 0.13 and 0.07, respectively. In the appropriateness for the interlocutor metric, only the **NA** condition has significantly higher scores than ours. Furthermore, as shown in Figure 2(b), the blue bar region indicates a higher proportion of participants choosing the correctly matched motion as their preference. We believe that several factors contribute to these results. Firstly, we make effective use of the provided information, including audio, transcribed text, and the interlocutor's behavior. Our data processing methods have demonstrated their effectiveness. Additionally, the introduced cross-modal attention encoder proves to be effective. It enables us to adequately encode information from different modalities, thus allowing the interlocutor's behavior to influence the generation of the main agent's motions.

We also achieve unsatisfactory results in the human-likeness metric, with a score of only 24. This is mainly because of the limitations inherent from the diffusion models, we can only generate motion sequences of a fixed length about 300 frames. This results in noticeable jitter at the junctions of different motion segments, despite introducing the previous pose as part of the generation condition to mitigate this issue. Furthermore, we attempt to incorporate acceleration between adjacent frames to constrain the model and increase the length of generated sequences while reducing the discontinuities in the joints. However, these methods do not yield the expected results. The acceleration constraint reduces the richness of the generated motions, making them less human-like. Directly increasing the generation length leads to significant jitter in the generated gesture motions.

6 CONCLUSION

We propose the DiffuGesture as described in this paper to participate in the GENEA Challenge 2023. Based on conditional diffusion models, we develop a system that generates co-speech human gestures for the main agent in the two-person dialogue. In our system, we encode the features of audio, transcriptions, interlocutor behavior using a transformer encoder. Furthermore, we adopt a

classifier-free guidance to trade off between diversity and gesture quality. The evaluation results show that DiffuGesture performs well in terms of appropriateness for the interlocutor metric. However, compared to other systems participating in the challenge, it dose not generate high-fidelity human-like motions effectively.

In the future, we will continue to explore conditional diffusion models to generate high-fidelity co-speech human gestures in various scenarios. We aim to handle the generation of variable-length motion sequences and reduce the distortion of motions at breakpoints. Additionally, we intend to investigate the incorporation of semantic supervision to aid in the generation of co-speech gestures. We will focus on these aspects in our future work.

REFERENCES

[1] Simon Alexanderson, Rajmund Nagy, Jonas Beskow, and Gustav Eje Henter. 2022. Listen, denoise, action! Audio-driven motion synthesis with diffusion models. *arXiv preprint arXiv:2211.09707* (2022).

[2] Tenglong Ao, Qingzhe Gao, Yuke Lou, Baoquan Chen, and Libin Liu. 2022. Rhythmic gesticulator: Rhythm-aware co-speech gesture synthesis with hierarchical neural embeddings. *ACM Transactions on Graphics (TOG)* 41, 6 (2022), 1–19.

[3] Uttaran Bhattacharya, Nicholas Rewkowski, Abhishek Banerjee, Pooja Guhan, Aniket Bera, and Dinesh Manocha. 2021. Text2gestures: A transformer-based network for generating emotive body gestures for virtual agents. In *2021 IEEE virtual reality and 3D user interfaces (VR)*. IEEE, 1–10.

[4] Che-Jui Chang, Sen Zhang, and Mubbasir Kapadia. 2022. The IVI Lab entry to the GENEA Challenge 2022–A Tacotron2 based method for co-speech gesture generation with locality-constraint attention mechanism. In *Proceedings of the 2022 International Conference on Multimodal Interaction*. 784–789.

[5] Prafulla Dhariwal and Alexander Nichol. 2021. Diffusion models beat gans on image synthesis. *Advances in neural information processing systems* 34 (2021), 8780–8794.

[6] S. Ginosar, A. Bar, G. Kohavi, C. Chan, A. Owens, and J. Malik. 2019. Learning Individual Styles of Conversational Gesture. In *Computer Vision and Pattern Recognition (CVPR)*. IEEE.

[7] William Harvey, Saeid Naderiparizi, Vaden Masrani, Christian Weilbach, and Frank Wood. 2022. Flexible diffusion modeling of long videos. *Advances in Neural Information Processing Systems* 35 (2022), 27953–27965.

[8] Jonathan Ho, Ajay Jain, and Pieter Abbeel. 2020. Denoising diffusion probabilistic models. *Advances in neural information processing systems* 33 (2020), 6840–6851.

[9] Jonathan Ho and Tim Salimans. 2022. Classifier-free diffusion guidance. *arXiv preprint arXiv:2207.12598* (2022).

[10] Biao Jiang, Xin Chen, Wen Liu, Jingyi Yu, Gang Yu, and Tao Chen. 2023. MotionGPT: Human Motion as a Foreign Language. *arXiv preprint arXiv:2306.14795* (2023).

[11] Diederik P Kingma and Max Welling. 2013. Auto-encoding variational bayes. *arXiv preprint arXiv:1312.6114* (2013).

[12] Taras Kucherenko, Patrik Jonell, Sanne Van Waveren, Gustav Eje Henter, Simon Alexandersson, Iolanda Leite, and Hedvig Kjellström. 2020. Gesticulator: A framework for semantically-aware speech-driven gesture generation. In *Proceedings of the 2020 International Conference on Multimodal Interaction*. 242–250.

[13] Taras Kucherenko, Patrik Jonell, Youngwoo Yoon, Pieter Wolfert, Zerrin Yumak, and Gustav Henter. 2021. GENEA Workshop 2021: The 2nd Workshop on Generation and Evaluation of Non-verbal Behaviour for Embodied Agents. In *Proceedings of the 2021 International Conference on Multimodal Interaction*. 872–873.

[14] Taras Kucherenko, Rajmund Nagy, Youngwoo Yoon, Jieyeon Woo, Teodor Nikolov, Mihail Tsakov, and Gustav Eje Henter. 2023. The GENEA Challenge 2023: A large-scale evaluation of gesture generation models in monadic and dyadic settings. In *Proceedings of the ACM International Conference on Multimodal Interaction (ICMI '23)*. ACM.

[15] Gilwoo Lee, Zhiwei Deng, Shugao Ma, Takaaki Shiratori, Siddhartha S Srinivasa, and Yaser Sheikh. 2019. Talking with hands 16.2 m: A large-scale dataset of synchronized body-finger motion and audio for conversational motion analysis and synthesis. In *Proceedings of the IEEE/CVF International Conference on Computer Vision*. 763–772.

[16] Sergey Levine, Philipp Krähenbühl, Sebastian Thrun, and Vladlen Koltun. 2010. Gesture controllers. In *Acm siggraph 2010 papers*. 1–11.

[17] Buyu Li, Yongchi Zhao, Shi Zhelun, and Lu Sheng. 2022. Danceformer: Music conditioned 3d dance generation with parametric motion transformer. In *Proceedings of the AAAI Conference on Artificial Intelligence*, Vol. 36. 1272–1279.

[18] Jing Li, Di Kang, Wenjie Pei, Xuefei Zhe, Ying Zhang, Zhenyu He, and Linchao Bao. 2021. Audio2gestures: Generating diverse gestures from speech audio with conditional variational autoencoders. In *Proceedings of the IEEE/CVF International Conference on Computer Vision*. 11293–11302.

[19] Xian Liu, Qianyi Wu, Hang Zhou, Yinghao Xu, Rui Qian, Xinyi Lin, Xiaowei Zhou, Wayne Wu, Bo Dai, and Bolei Zhou. 2022. Learning Hierarchical Cross-Modal Association for Co-Speech Gesture Generation. In *Proceedings of the IEEE/CVF Conference on Computer Vision and Pattern Recognition*. 10462–10472.

[20] Shuhong Lu and Andrew Feng. 2022. The DeepMotion entry to the GENEA Challenge 2022. In *Proceedings of the 2022 International Conference on Multimodal Interaction*. 790–796.

[21] Steven G McCafferty. 2004. Space for cognition: Gesture and second language learning. *International Journal of Applied Linguistics* 14, 1 (2004), 148–165.

[22] Shenhan Qian, Zhi Tu, Yihao Zhi, Wen Liu, and Shenghua Gao. 2021. Speech drives templates: Co-speech gesture synthesis with learned templates. In *Proceedings of the IEEE/CVF International Conference on Computer Vision*. 11077–11086.

[23] Alec Radford, Jong Wook Kim, Chris Hallacy, Aditya Ramesh, Gabriel Goh, Sandhini Agarwal, Girish Sastry, Amanda Askell, Pamela Mishkin, Jack Clark, et al. 2021. Learning transferable visual models from natural language supervision. In *International conference on machine learning*. PMLR, 8748–8763.

[24] Nataniel Ruiz, Yuanzhen Li, Varun Jampani, Yael Pritch, Michael Rubinstein, and Kfir Aberman. 2023. Dreambooth: Fine tuning text-to-image diffusion models for subject-driven generation. In *Proceedings of the IEEE/CVF Conference on Computer Vision and Pattern Recognition*. 22500–22510.

[25] Najmeh Sadoughi and Carlos Busso. 2018. Novel realizations of speech-driven head movements with generative adversarial networks. In *2018 IEEE International Conference on Acoustics, Speech and Signal Processing (ICASSP)*. IEEE, 6169–6173.

[26] Guy Tevet, Brian Gordon, Amir Hertz, Amit H Bermano, and Daniel Cohen-Or. 2022. Motionclip: Exposing human motion generation to clip space. In *European Conference on Computer Vision*. Springer, 358–374.

[27] Guy Tevet, Sigal Raab, Brian Gordon, Yonatan Shafir, Daniel Cohen-Or, and Amit H Bermano. 2022. Human motion diffusion model. *arXiv preprint arXiv:2209.14916* (2022).

[28] Ashish Vaswani, Noam Shazeer, Niki Parmar, Jakob Uszkoreit, Llion Jones, Aidan N Gomez, Łukasz Kaiser, and Illia Polosukhin. 2017. Attention is all you need. *Advances in neural information processing systems* 30 (2017).

[29] Petra Wagner, Zofia Malisz, and Stefan Kopp. 2014. Gesture and speech in interaction: An overview. , 209–232 pages.

[30] Bowen Wu, Chaoran Liu, Carlos Toshinori Ishi, and Hiroshi Ishiguro. 2021. Modeling the conditional distribution of co-speech upper body gesture jointly using conditional-GAN and unrolled-GAN. *Electronics* 10, 3 (2021), 228.

[31] Jamie Wynn and Daniyar Turmukhambetov. 2023. Diffusionerf: Regularizing neural radiance fields with denoising diffusion models. In *Proceedings of the IEEE/CVF Conference on Computer Vision and Pattern Recognition*. 4180–4189.

[32] Lianying Yin, Yijun Wang, Tianyu He, Jinming Liu, Wei Zhao, Bohan Li, Xin Jin, and Jianxin Lin. 2023. EMoG: Synthesizing Emotive Co-speech 3D Gesture with Diffusion Model. *arXiv preprint arXiv:2306.11496* (2023).

[33] Youngwoo Yoon, Bok Cha, Joo-Haeng Lee, Minsu Jang, Jaeyeon Lee, Jaehong Kim, and Geehyuk Lee. 2020. Speech Gesture Generation from the Trimodal Context of Text, Audio, and Speaker Identity. *ACM Transactions on Graphics* 39, 6 (2020).

[34] Youngwoo Yoon, Woo-Ri Ko, Minsu Jang, Jaeyeon Lee, Jaehong Kim, and Geehyuk Lee. 2019. Robots learn social skills: End-to-end learning of co-speech gesture generation for humanoid robots. In *2019 International Conference on Robotics and Automation (ICRA)*. IEEE, 4303–4309.

[35] Youngwoo Yoon, Pieter Wolfert, Taras Kucherenko, Carla Viegas, Teodor Nikolov, Mihail Tsakov, and Gustav Eje Henter. 2022. The GENEA Challenge 2022: A large evaluation of data-driven co-speech gesture generation. In *Proceedings of the 2022 International Conference on Multimodal Interaction*. 736–747.

[36] Jianrong Zhang, Yangsong Zhang, Xiaodong Cun, Shaoli Huang, Yong Zhang, Hongwei Zhao, Hongtao Lu, and Xi Shen. 2023. T2m-gpt: Generating human motion from textual descriptions with discrete representations. *arXiv preprint arXiv:2301.06052* (2023).

[37] Mingyuan Zhang, Zhongang Cai, Liang Pan, Fangzhou Hong, Xinying Guo, Lei Yang, and Ziwei Liu. 2022. Motiondiffuse: Text-driven human motion generation with diffusion model. *arXiv preprint arXiv:2208.15001* (2022).

[38] Chi Zhou, Tengyue Bian, and Kang Chen. 2022. Gesturemaster: Graph-based speech-driven gesture generation. In *Proceedings of the 2022 International Conference on Multimodal Interaction*. 764–770.

[39] Lingting Zhu, Xian Liu, Xuanyu Liu, Rui Qian, Ziwei Liu, and Lequan Yu. 2023. Taming Diffusion Models for Audio-Driven Co-Speech Gesture Generation. In *Proceedings of the IEEE/CVF Conference on Computer Vision and Pattern Recognition (CVPR)*. 10544–10553.

A RESEARCH METHODS

A.1 Significant differences for Appropriateness

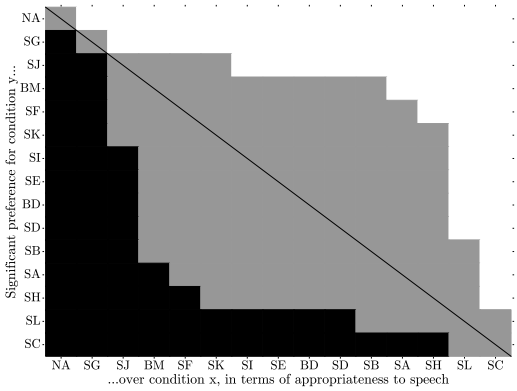

(a) Appropriateness for agent speech

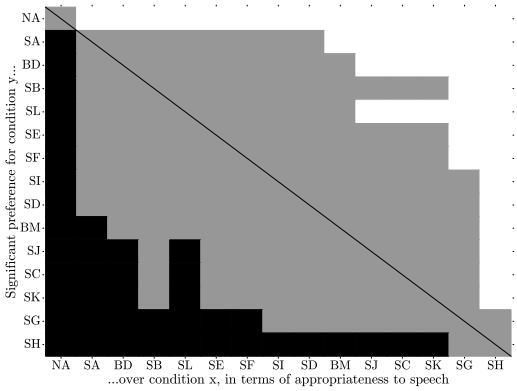

(b) Appropriateness for the interlocutor

Figure 3: Significant differences between conditions in the two appropriateness studies. White means the condition listed on the y-axis achieved an MAS significantly above the condition on the x-axis, black means the opposite (y scored below x), and grey means no statistically significant difference at level $\alpha = 0.5$ after correction for the false discovery rate.

A.2 Significant differences for Human-likeness

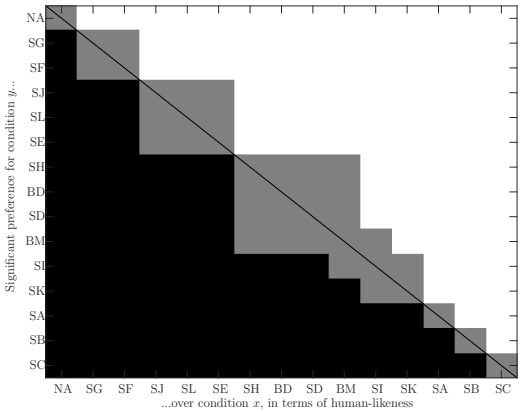

(a) Appropriateness for agent speech

Figure 4: Significance of pairwise differences between conditions. White means that the condition listed on the y-axis rated significantly above the condition on the x-axis, black means the opposite (y rated below x), and grey means no statistically significant difference at the level $\alpha = 0.05$ after Holm-Bonferroni correction.